

5549-1-P = RL-2125

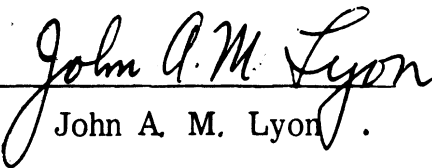
Bimonthly Report No. 1
January 3, 1963 to March 2, 1963

5549-1-P

STUDY AND INVESTIGATION OF A UHF-VHF ANTENNA

by

A. T. Adams
R. M. Kalafus

Approved by 
John A. M. Lyon .

COOLEY ELECTRONICS LABORATORY

Department of Electrical Engineering
The University of Michigan
Ann Arbor

United States Air Force
Air Force Systems Command
Aeronautical Systems Division
Contract No. AF 33(657)-10607
Wright-Patterson Air Force Base, Ohio

May 1963

**MISSING
PAGE**

TABLE OF CONTENTS

	<u>Page</u>
LIST OF ILLUSTRATIONS	iv
ABSTRACT	v
1. REPORTS, TRAVEL, AND VISITORS	1
2. FACTUAL DATA	2
2.1 Rectangular Cavity Variational Results	2
2.2 Rectangular Cavity Experimental Results	3
2.3 Rectangular Cavity Equivalent Circuit Methods and Application to Cavity Design and Bandwidth Prediction	7
2.4 Verification of Variational Data	11
2.5 Efficiency of a Rectangular Cavity Slot Radiator	14
2.5.1 General Formulation	14
2.5.2 Efficiency Using High Q Material	23
2.5.3 Efficiency with Probe Near Aperture	25
2.6 Design of Wideband Antenna Utilizing Ferrite	27
3. ACTIVITIES FOR NEXT PERIOD	29
4. SUMMARY	30
REFERENCES	31

LIST OF ILLUSTRATIONS

<u>Figure</u>	<u>Title</u>	<u>Page</u>
1	(a) Rectangular waveguide slot radiator loaded with isotropic ferrite material, (b) equivalent circuit.	3
2	Aperture admittance of a loaded waveguide radiator.	4
3	Rectangular cavity slot antenna.	6
4	Rectangular cavity with cylindrical probe.	6
5	Rectangular cavity with T-Bar feed.	8
6	Experimental setup for slot measurements.	8
7	Aperture admittance of a loaded rectangular waveguide radiator; (a) $\mu = \epsilon = 3$, (b) $\mu = 1$, $\epsilon = 10$, (c) $\mu = 10$, $\epsilon = 1$.	9
8	Comparison of experimental data on BW + short position with Smith Chart calculations.	12
9	Dielectric loaded waveguide radiator; (a) front view, (b) back view.	13
10	Slotted dielectric and wedges.	13
11	(a) Efficiency of a rectangular cavity slot radiator, (b) efficiency of a rectangular cavity slot radiator.	14

ABSTRACT

Theoretical curves for the real and imaginary parts of the aperture admittance of a loaded rectangular waveguide radiator are given, for various values of μ , ϵ , frequency, and b/a ratio. The data shown have been computed using the variational expression for aperture admittance previously derived in QPR No. 9.

Data are presented on the bandwidth characteristics of a rectangular cavity slot antenna loaded with ferrite powder, as a function of short position, feed arrangement, and frequency.

A simple equivalent circuit derived from the variational data is used to calculate bandwidth and short position as a function of frequency. Data obtained from this model are compared with experimental results. The efficiency of the rectangular cavity slot antenna is calculated using the variational data.

Plans for traveling wave antenna experiments are described.

1. REPORTS, TRAVEL, AND VISITORS

During this period no reports were issued, and no one visited the project.

On January 24, 1963, Dr. John A. M. Lyon visited the Aeronautical Systems Division of Wright-Patterson Air Force Base to discuss the results, progress, and further plans for these studies.

2. FACTUAL DATA

2.1 Rectangular Cavity Variational Results

A stationary expression for the aperture admittance of a loaded waveguide radiator (Fig. 1) was formulated in QPR No. 9 (formula 8, p. 17). The expression was then expanded into the form shown on p. 28 of QPR No. 9, the first term of which represents the dominant mode approximation to the aperture field.

Dominant Mode Approximation:

$$\begin{aligned}
 Y &= G + jB \\
 &= -\frac{4\mu_r}{\Gamma_{10}ab} \left\{ \int_0^a \int_0^b (b - \sigma) \left[(a - \lambda) \left(k_0^2 - \frac{\pi^2}{a^2} \right) \cos \frac{\pi\lambda}{a} \right. \right. \\
 &\quad \left. \left. + \frac{a}{\pi} \left(k_0^2 + \frac{\pi^2}{a^2} \right) \sin \frac{\pi\lambda}{a} \right] \frac{e^{-jk_0 \sqrt{\lambda^2 + \sigma^2}}}{2\pi \sqrt{\lambda^2 + \sigma^2}} d\sigma d\lambda \right\}
 \end{aligned}$$

It may be noted that the integral is a function only of the product $\mu_r \epsilon_r$ since $k_0 = \frac{k}{\sqrt{\mu_r \epsilon_r}}$. Thus the basic data can be expressed in terms of three parameters ka , b/a , $\mu_r \epsilon_r$ and results can be expanded for particular values of μ_r by multiplication. This also indicates that, for a specified $\mu_r \epsilon_r$ product, the effect of using materials with μ_r greater than one is primarily to increase the magnitudes of B and G. The ratio B/G is unchanged. The reflection coefficient depends primarily on the ratio B/G, although it is decreased somewhat by using μ_r greater than one. This first term involving a double integration was evaluated by computer. The evaluation involves an integral with a singularity. The integral was split into two parts which were evaluated separately and then added. As a check on the computation, two different increments were used in the integration and their results compared. The maximum error in the imaginary part of the admittance was .7 percent. The integration in G involves positive and negative parts which nearly cancel as the $\mu_r \epsilon_r$ product becomes large. Correspondingly the error in the real part of the admittance increased to a

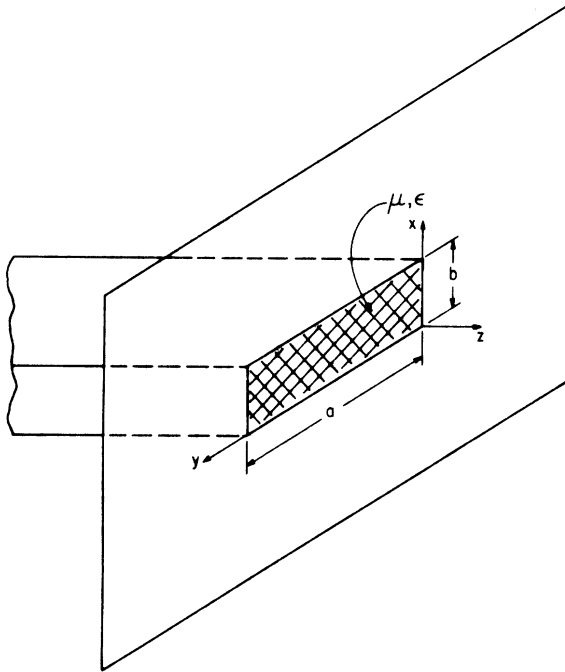


Fig. 1(a). Rectangular waveguide slot radiator loaded with isotropic ferrite material.

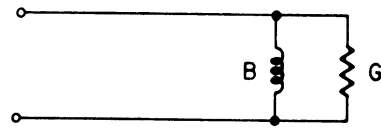


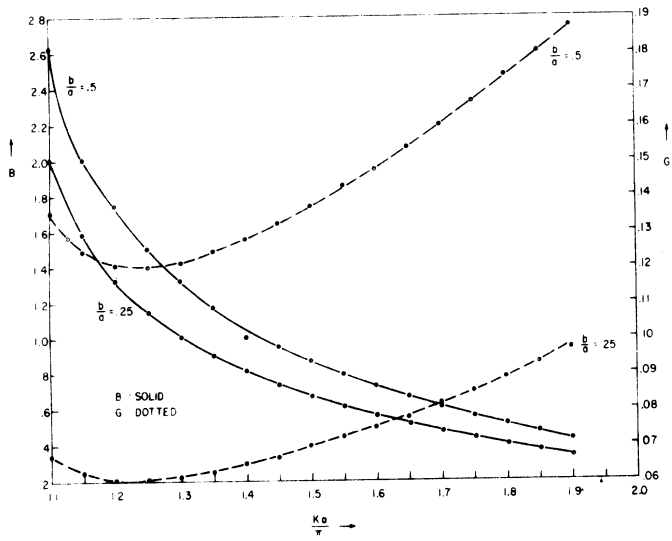
Fig. 1(b). Equivalent circuit.

maximum of 2.5 percent at $\mu_r = \epsilon_r = 10$. Asymptotic formulas were developed to give the values of G for $\mu_r \epsilon_r$ products greater than 100. The details of these calculations will be given in a later report.

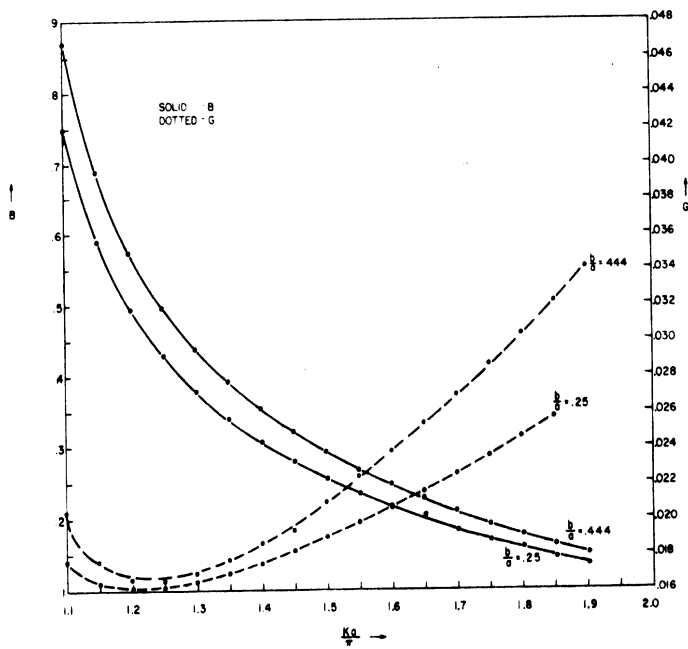
The results of the computation are shown in Fig. 2. It is estimated that the computation is accurate to within a few percent.

2.2 Rectangular Cavity Experimental Results

Experimental work on the loaded rectangular slot antenna has concentrated on the bandwidth characteristics as a function of location and type of feed and short position. Types of feed tested includes several types of cylindrical probes, ball probes and T-bar probes. Figure 3 shows the rectangular cavity slot antenna and Figs. 4 and 5 show typical feed arrangements. The aperture dimensions are 3" x 11-3/4" and the cavity length varies throughout the experiments. Data on bandwidth as a function of frequency, short position, and feed arrangement are shown in Table I. The experimental setup shown in Fig. 6 was used to locate resonance and adjust for maximum bandwidth. The envelope of the scope display is proportional to the reflection coefficient. This method allows rapid location of the resonance point. Once the resonance was located, more accurate data was taken using a PRD standing wave detector. Some of the general results are summarized below.



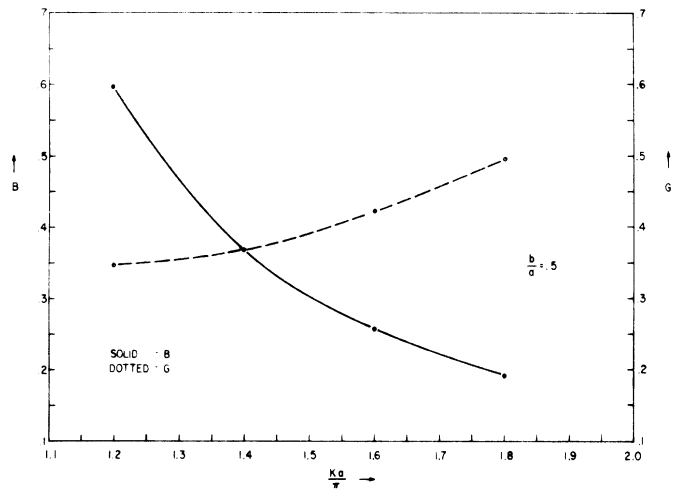
(a) $\mu = \epsilon = 3$



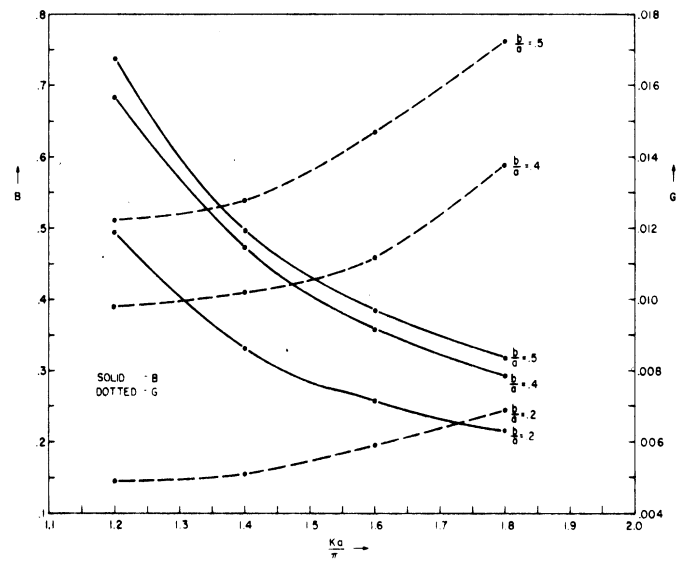
(b) $\mu = 1, \epsilon = 10$

Fig. 2. Aperture admittance of a loaded waveguide radiator.

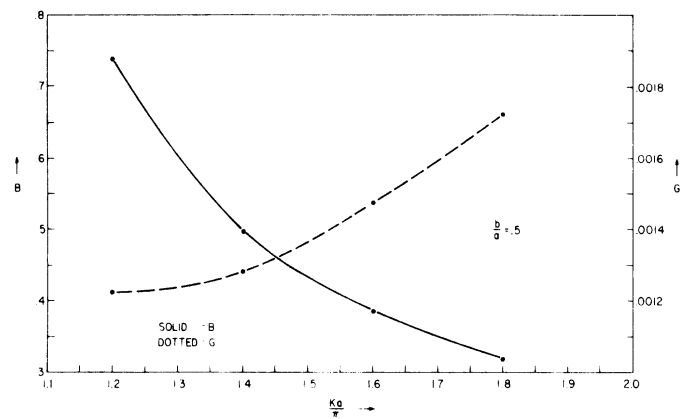
(c) $\mu = 10, \epsilon = 1$



(d) $\mu = \epsilon = 10$



(e) $\mu = 1, \epsilon = 100$



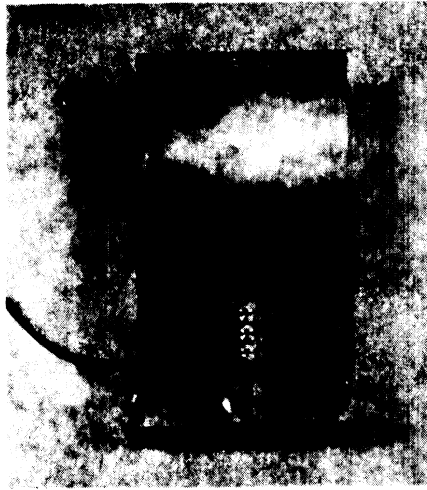


Fig. 3. Rectangular cavity slot antenna.

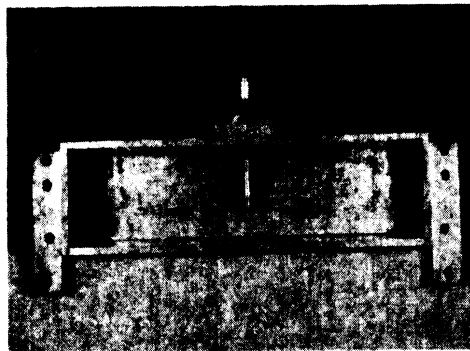


Fig. 4. Rectangular cavity with cylindrical probe.

1. $1/2''$, $1/4''$, and $1/8''$ diameter cylindrical probes were used. Bandwidth was not significantly changed by a change in probe diameter or the use of ball probes.

2. Minimum VSWR occurred for a probe insertion of $1-1/2''$ to $2''$. The adjustment of probe depth was relatively critical. The reason for this is that the shunt conductance introduced into the cavity varies rapidly with probe insertion.

3. Probe location with respect to the short position was not critical. In most cases the probe was located approximately halfway between the short and the aperture. At the higher frequencies, it was necessary to locate the probe closer to the aperture as the distance in wavelengths from the aperture to the short decreases.

<u>Center Frequency</u>	<u>Bandwidth</u>	<u>Short Location</u>	<u>Probe Location (Distance from Aperture)</u>	<u>Probe Depth</u>	<u>Probe</u>
215 Mc	3 Mc	9-1/2"	5-1/2"	2"	C. P.
217 Mc	4 Mc	9-1/2"	5-1/2"	1-27/32"	C. P.
225 Mc	6 Mc	8-1/2"	5-1/2"	2"	C. T.
230 Mc	9 Mc	9-1/2"	5-1/2"	1"	T. B.
239 Mc	7 Mc	7-1/2"	3-1/2"	1-3/4"	C. T.
249 Mc	7 Mc	6-1/2"	2-1/2"	1-21/32"	C. T.
251 Mc	8 Mc	6"	2-1/2"	1-23/32"	C. T.
253 Mc	9 Mc	6"	2-1/2"	2"	C. T.
254 Mc	10 Mc	6"	2-1/2"	2"	C. T.
281 Mc	9 Mc	5"	2-1/2"	1-3/4"	C. T.
286 Mc	10 Mc	4"	1/2"	1-11/16"	C. T.
298 Mc	16 Mc	4"	1/2"	1-3/4"	C. T.
305 Mc	16 Mc	4"	1/2"	1-1/2"	C. T.
312 Mc	15 Mc	4"	1-1/2"	1-21/32"	C. T.
318 Mc	20 Mc	4"	1-1/2"	1-3/16"	T. B.
326 Mc	20 Mc	4"	3-1/2"	2-13/16"	C. T.
330 Mc	32 Mc	4"	2-1/2"	1-1/4"	T. B.
357 Mc	33 Mc	4"	2-1/2"	3"	C. T.
383 Mc	36 Mc	4"	2-1/2"	1-13/16"	C. T.
431 Mc	43 Mc	4"	1-1/2"	2-7/32"	T. B.
502 Mc	114 Mc	2"	1-1/2"	2"	C. T.

Table I. Results of ferrite powder loaded rectangular cavity experiments. Bandwidth is based on VSWR = 3.0.

C. P. = Cylindrical probe

T. B. = T-Bar

4. Most of the tests conducted were with cylindrical probes because of the ease of adjustment. Some of the tests with T-bar probes indicated significant improvement in bandwidth.

2.3 Rectangular Cavity Equivalent Circuit Methods and Application to Cavity Design and Bandwidth Prediction

The model for the variational study involves an infinitely long waveguide. However, the use of a simple equivalent circuit permits one to take the finite length of the

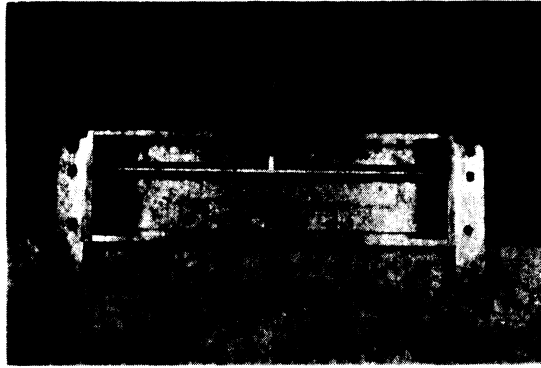


Fig. 5. Rectangular cavity with T-Bar feed.

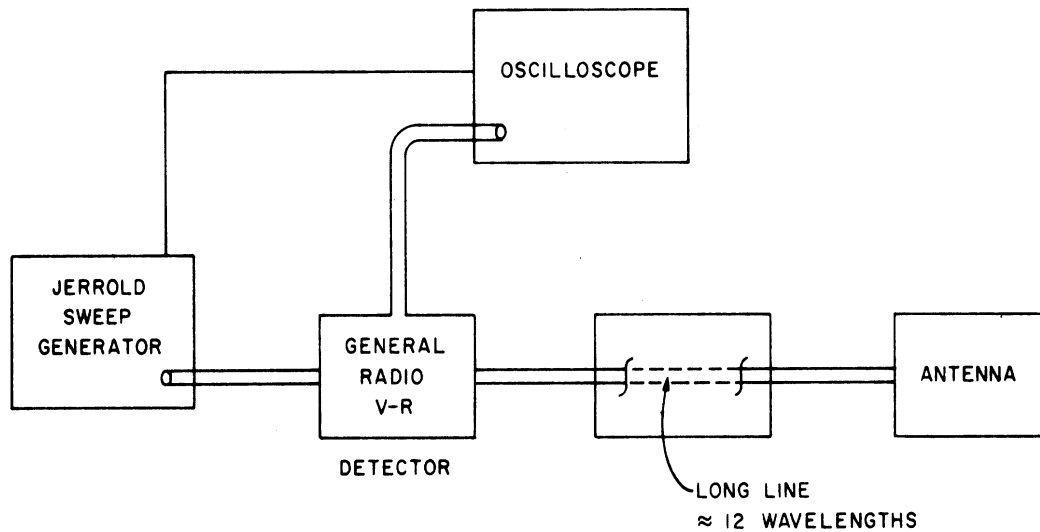


Fig. 6. Experimental setup for slot measurements.

cavity into account. Early in the experimental work it was noted that the feed arrangement (feed location, probe depth, and probe size) had little effect on the resonant frequency. This suggested that the resonant frequency could be predicted from a consideration of the aperture admittance and the short position alone. Furthermore, since the aperture admittance varies rapidly with frequency, it might be expected that the dominant effect in determining bandwidth would be the variation with frequency of the reactance of the aperture admittance and the short reactance. Theoretical data for short position and bandwidth as a function of μ , ϵ , b/a and frequency was calculated. The theoretical aperture admittance data was plotted on Smith Charts (Fig. 7), the short was located for resonance at a given frequency (Table II), and the half power bandwidth (Table III) was calculated using successive approximations on the Smith

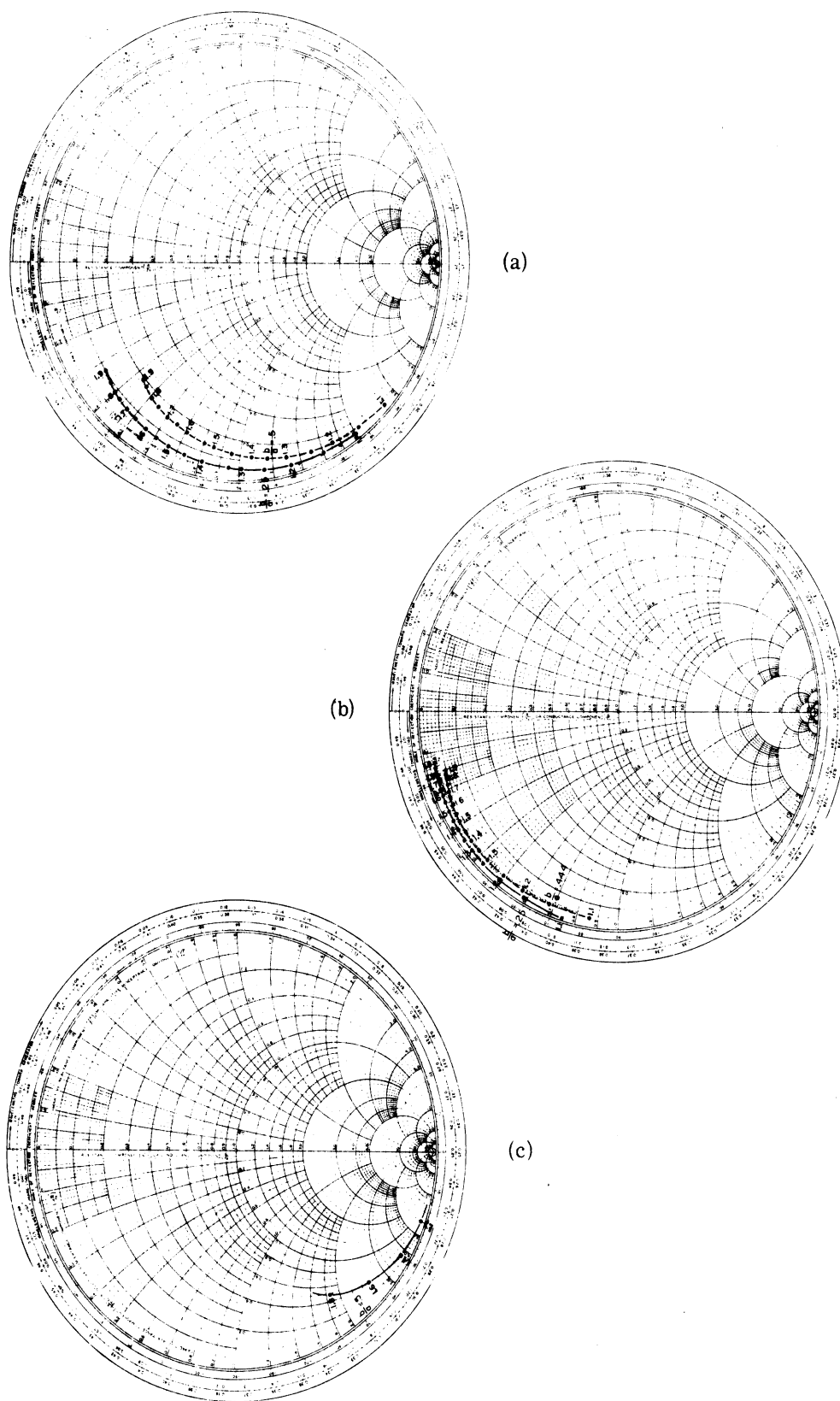


Fig. 7. Aperture admittance of a loaded rectangular waveguide radiator; (a) $\mu = \epsilon = 3$, (b) $\mu = 1$, $\epsilon = 10$, (c) $\mu = 10$, $\epsilon = 1$.

$\frac{ka}{\pi}$	$\mu = 1$			$\mu = 3$		$\mu = 10$			
	$\epsilon = 10$		$\epsilon = 100$	$\epsilon = 3$		$\epsilon = 1$	$\epsilon = 10$		
	b/a = 0.250	b/a = 0.444	b/a = 0.500	b/a = 0.250	b/a = 0.500	b/a = 0.500	b/a = 0.200	b/a = 0.400	b/a = 0.500
1.10	0.352	0.363		0.426	0.442				
1.15	0.335	0.345		0.411	0.429				
1.20	0.323	0.333	0.361	0.397	0.418	0.474	0.469	0.476	0.479
1.25	0.314	0.323		0.386	0.407				
1.30	0.307	0.314		0.376	0.396				
1.35	0.302	0.309		0.311	0.388				
1.40	0.298	0.304	0.323	0.359	0.381	0.459	0.453	0.465	0.469
1.45	0.294	0.300		0.351	0.372				
1.50	0.291	0.294		0.343	0.363				
1.55	0.286	0.291		0.338	0.359				
1.60	0.284	0.288	0.308	0.332	0.349	0.442	0.441	0.456	0.460
1.65	0.281	0.285		0.325	0.343				
1.70	0.278	0.282		0.320	0.338				
1.75	0.277	0.280		0.315	0.332				
1.80	0.275	0.278	0.298	0.311	0.326	0.425	0.405	0.447	0.451
1.85	0.273	0.276		0.306	0.320				
1.90	0.271	0.274		0.301	0.316				

Table II. Short position in (wavelengths) from aperture.

Chart, taking into account both the variation of the aperture admittance and the variation of the short reactance. For simplicity, half power bandwidths were calculated (VSWR = 6.0).

It should be noted that the experimental data for bandwidth in Table I corresponds to a VSWR of 3.0. Multiplying the bandwidth by a factor of .7 gives the approximate bandwidths for a VSWR of 3.0. This factor was used in comparing experimental and theoretical data in Fig. 8. Figure 8 shows comparison of the experimental data for the ferrite loaded slot antenna with theoretical data on short position and bandwidth for $\mu = \epsilon = 3$. As is shown by the data, agreement is fairly good, although the μ and ϵ of the powder material is not known very accurately.

The experimental short position data differs from the theoretical data by 10-20 percent. Over half of the experimental bandwidth data points lie within 10 percent of

μ	ϵ	b/a	ka/ π	BW
1	10	0.250	1.1	.85
			1.3	1.98
			1.5	3.15
			1.7	4.54
			1.9	5.85
		0.444	1.1	2.12
			1.3	4.27
			1.5	4.94
			1.7	6.69
			1.9	8.85
3	3	0.250	1.1	.79
			1.3	3.05
			1.5	5.68
			1.7	8.61
			1.9	12.10
		0.500	1.1	2.0
			1.3	5.85
			1.5	8.40
			1.7	13.58
			1.9	21.20
10	1	0.500	1.2	1.45
			1.4	2.30
			1.6	5.20
			1.8	10.20

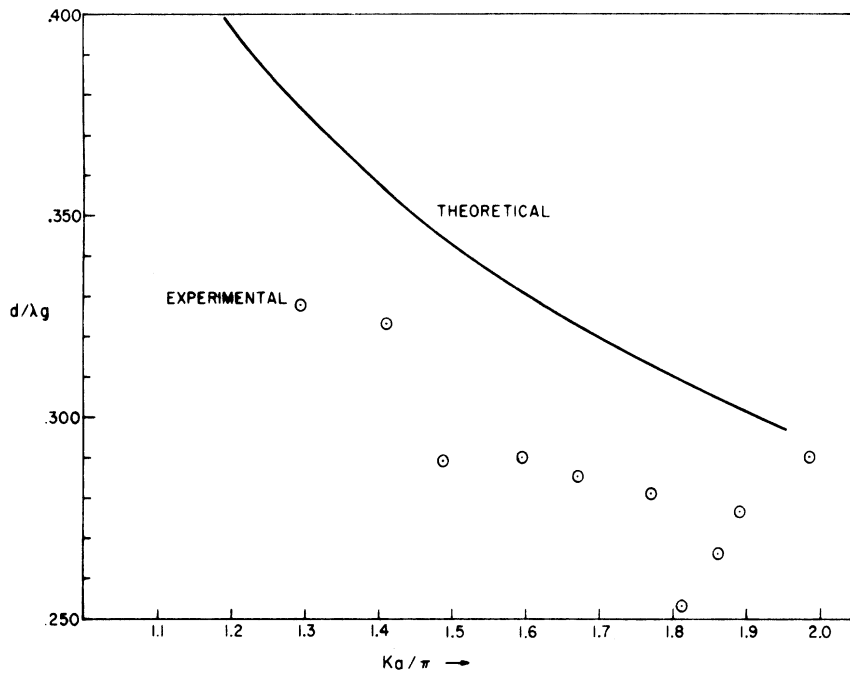
Table III. Bandwidth calculations.

the theoretical values. It is likely that further optimization would yield better agreement for the other points.

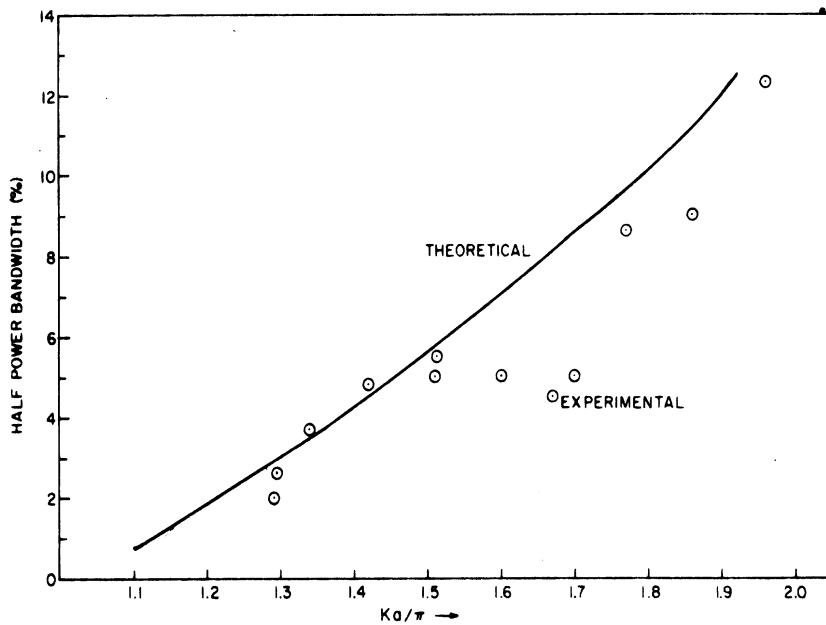
Since there is a relatively high reflection coefficient at the ferrite-air interface, the device resembles a resonant cavity and it would be expected that by methods of this sort, combined perhaps with standard perturbation methods to take into account the probe configuration, would yield accurate predictions of resonant frequency. Future tests with solid dielectric and solid ferrite material, whose characteristics can be accurately measured, will provide a further comparison of the theoretical methods with experimental results.

2.4 Verification of Variational Data

An experimental check on the variational data has begun. The equipment used in the experiment is shown in Figs. 9 and 10. A slotted dielectric block has been fitted to a slotted X Band waveguide. The dielectric material is Emerson and Cumming Stycast Hi-K



(a)



(b)

Fig. 8. Comparison of experimental data on BW + short position with Smith Chart calculations. (a) short position in wavelengths from aperture, (b) half power bandwidths of rectangular cavity slot antenna.

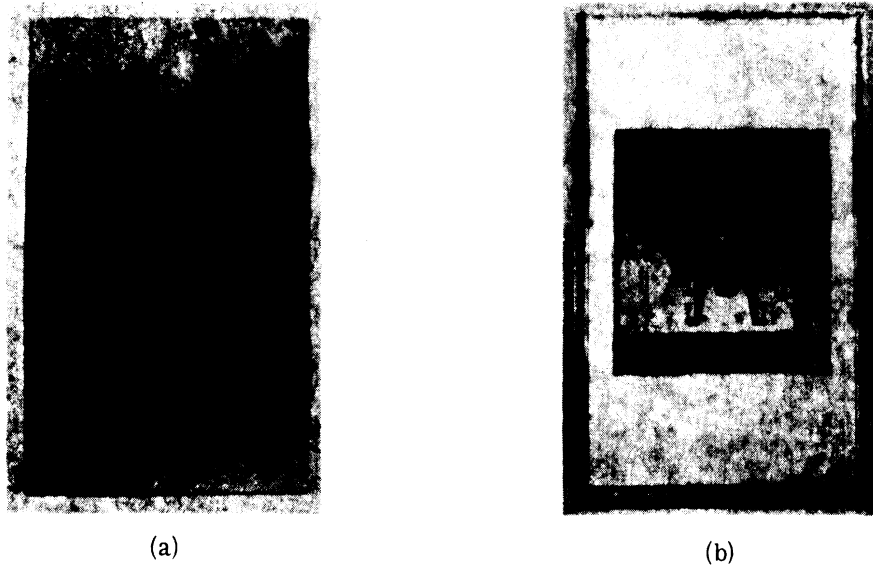


Fig. 9. Dielectric loaded waveguide radiator;
(a) front view, (b) back view.

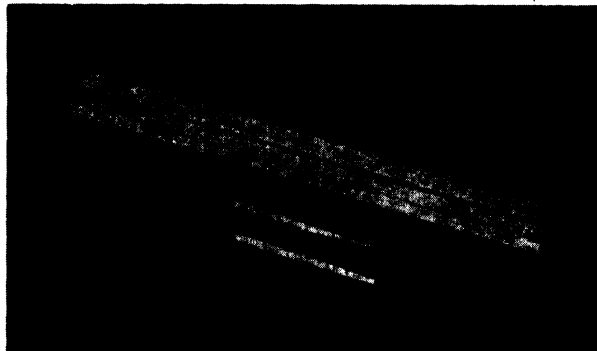


Fig. 10. Slotted dielectric and wedges.

with a dielectric constant of ten. The coaxial to waveguide adapter is also loaded with dielectric. The slot modifies the geometry somewhat so that the admittance measured does not correspond exactly to that formulated in the variational calculations. Tapered wedges (Fig. 10) which fit into the slot are used to provide a more accurate measurement of the VSWR of a geometry corresponding to the theoretical calculations. The dielectric loaded slotted line is mounted on a 2' x 3' ground plane. The ground plane will be mounted in the anechoic chamber and admittance measurements will be taken in the near future.

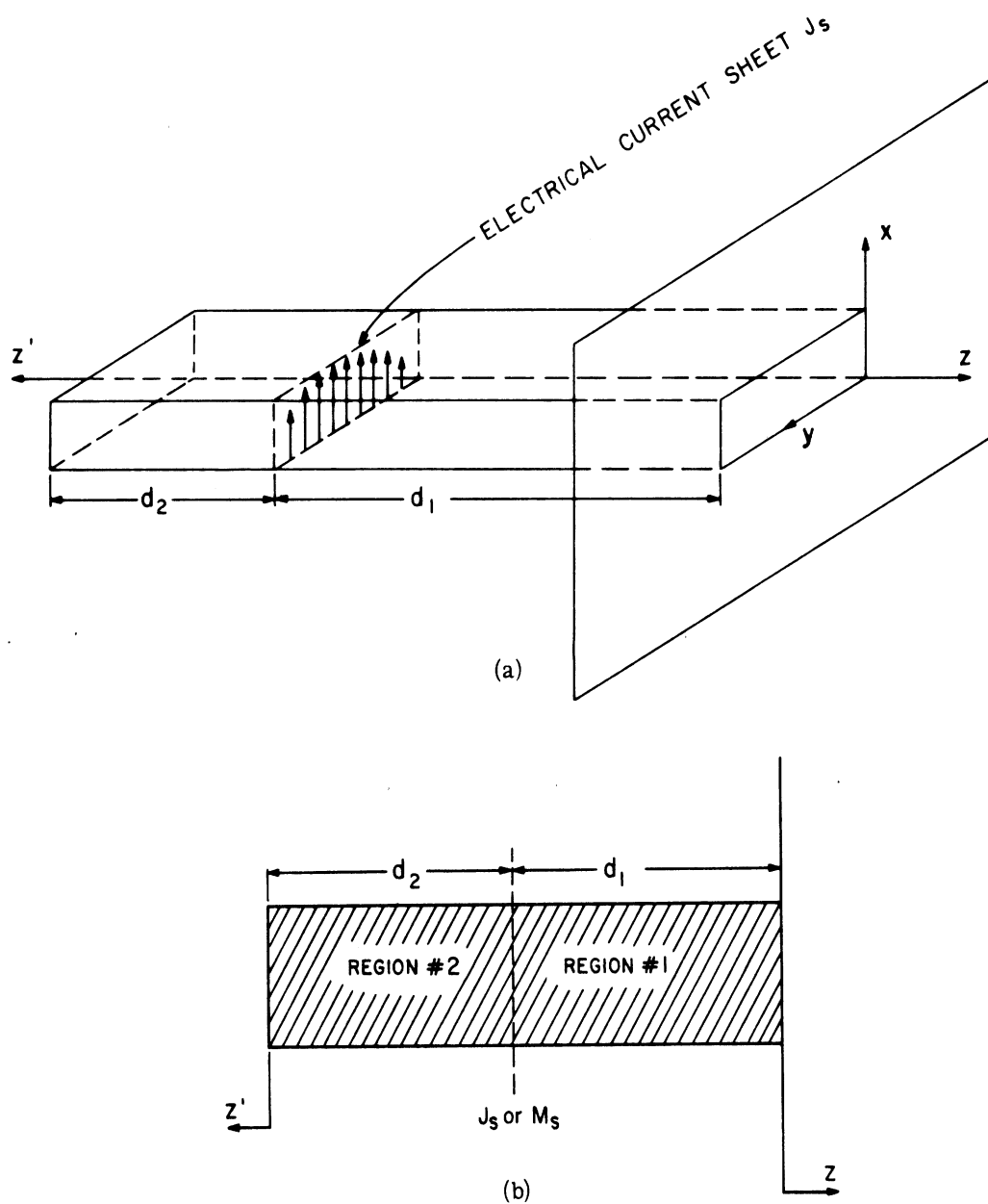


Fig. 11. (a) Efficiency of a rectangular cavity slot radiator, (b) efficiency of a rectangular cavity slot radiator.

2.5 Efficiency of a Rectangular Cavity Slot Radiator

2.5.1 General Formulation. The efficiency of a rectangular cavity slot radiator has been analyzed, assuming an attenuated dominant mode only in the cavity and utilizing the reflection coefficient at the aperture which has been evaluated by variational techniques. An electric current sheet source exciting the dominant mode is located at the probe position [Fig. 11(a) and (b)]. The source may also be assumed to be magnetic current, in

which case the complex constant A, which determines the fields in Region No. 2, will have a different value. The electric current source gives rise to a discontinuity in H_y whereas the magnetic current source produces a discontinuity in E_x . The radiated power is calculated by integrating Poynting's vector across the aperture. The formulation takes into account magnetic and electric volume losses and wall losses with certain simplifications resulting in special cases.

The fields are represented in terms of a Hertzian vector potential of magnetic type in Regions No. 1 and No. 2

$$\Pi_1^* = \frac{1}{j\omega\mu} \left[\frac{e^{-\Gamma_{10} z} - R e^{\Gamma_{10} z}}{\Gamma_{10}} \right] \sin \frac{\pi y}{a} \cdot \hat{y}$$

$$\Pi_2^* = \frac{A}{j\omega\mu} \left[\frac{e^{-\Gamma_{10} z'} + e^{\Gamma_{10} z'}}{\Gamma_{10}} \right] \sin \frac{\pi y}{a} \cdot \hat{y}$$

$$J_s = J_0 \sin \frac{\pi y}{a} \cdot \hat{x} \quad \text{electric current}$$

or

$$M_s = M_0 \sin \frac{\pi y}{a} \cdot \hat{y} \quad \text{magnetic current}$$

where:

R is the complex dominant mode reflection coefficient
evaluated in the variational calculations.

Efficiency

$$\text{time average power radiated} = \bar{P}_r = \text{Re} \int_0^a \int_0^b E_x H_y^* dx dy$$

(evaluated at $z = 0$)

time average power dissipation in the cavity

$$= \bar{P}_L = \int \int \int_{\text{cavity}} \omega \epsilon'' |E|^2 dv + \int \int \int_{\text{cavity}} \omega \mu'' |H|^2 dv$$

$$+ R_s \int \int \int_{\text{walls}} |H|^2 da$$

where E and H are rms values (Ref. 1).

$$\text{efficiency} = \frac{\bar{P}_r}{\bar{P}_r + \bar{P}_L} = \frac{1}{1 + \frac{\bar{P}_L}{\bar{P}_r}}$$

since we are concerned with the ratio \bar{P}_L/\bar{P}_r , it is immaterial whether we use peak or rms values in the above equations.

Solving for the Fields in Regions No. 1 and No. 2

$$\text{Let } \Gamma_{10} = \alpha_{10} + j\beta_{10}$$

Region No. 1:

$$E_{x1} = j\omega\mu \frac{\partial \Pi^*}{\partial z} = \left[e^{-\Gamma_{10}z} + R e^{\Gamma_{10}z} \right] \sin \frac{\pi y}{a}$$

$$H_{y1} = \left(\frac{\partial^2}{\partial y^2} + k^2 \right) \Pi^* = \frac{(k^2 a^2 - \pi^2)}{a^2} \left(-\frac{1}{j\omega\mu} \right) \left[\frac{e^{-\Gamma_{10}z} - R e^{\Gamma_{10}z}}{\Gamma_{10}} \right] \sin \frac{\pi y}{a}$$

$$H_{z1} = \frac{\partial^2 \Pi^*}{\partial y \partial z} = \left(\frac{1}{j\omega\mu} \right) \left(\frac{\pi}{a} \right) \left[e^{-\Gamma_{10}z} + R e^{\Gamma_{10}z} \right] \cos \frac{\pi y}{a}$$

Region No. 2:

$$E_{x2} = A \left[e^{-\Gamma_{10}z'} - e^{\Gamma_{10}z'} \right] \sin \frac{\pi y}{a}$$

$$H_{y2} = A \left(\frac{k^2 a^2 - \pi^2}{a^2} \right) \left(\frac{-1}{j\omega\mu} \right) \left[\frac{e^{-\Gamma_{10}z'} + e^{\Gamma_{10}z'}}{\Gamma_{10}} \right] \sin \frac{\pi y}{a}$$

$$H_{z2} = \left(\frac{1}{j\omega\mu} \right) \left(\frac{\pi}{a} \right) \left[e^{-\Gamma_{10}z'} - e^{\Gamma_{10}z'} \right] \cos \frac{\pi y}{a}$$

$$\begin{aligned}
|E_{x1}|^2 &= \sin^2 \frac{\pi y}{a} \left[e^{-2\alpha_{10}z} + |R|^2 e^{2\alpha_{10}z} + 2|R| \cos(2\beta_{10}z + \theta_r) \right] \\
|H_{y1}|^2 &= \left| \frac{k^2 a^2 - \pi^2}{\omega \mu a^2} \right|^2 \sin^2 \frac{\pi y}{a} \frac{1}{|\Gamma_{10}|^2} \\
&\quad \left[e^{-2\alpha_{10}z} + |R|^2 e^{2\alpha_{10}z} - 2|R| \cos(2\beta_{10}z + \theta_r) \right] \\
|H_{z1}|^2 &= \left| \frac{\pi}{a\omega\mu} \right|^2 \cos^2 \frac{\pi y}{a} \\
&\quad \left[e^{-2\alpha_{10}z} + |R|^2 e^{2\alpha_{10}z} + 2|R| \cos(2\beta_{10}z + \theta_r) \right]
\end{aligned}
\quad \left. \vphantom{\begin{aligned} |E_{x1}|^2 \\ |H_{y1}|^2 \\ |H_{z1}|^2 \end{aligned}} \right\} \text{Region No. 1}$$

$$\begin{aligned}
|E_{x2}|^2 &= |A^2| \sin^2 \left[e^{-2\alpha_{10}z'} + e^{2\alpha_{10}z'} - 2 \cos 2\beta_{10}z' \right] \\
|H_{y2}|^2 &= \left| \frac{k^2 a^2 - \pi^2}{\omega \mu a^2} \right|^2 \frac{|A^2|}{|\Gamma_{10}|^2} \sin^2 \frac{\pi y}{a} \\
&\quad \left[e^{-2\alpha_{10}z'} + e^{2\alpha_{10}z'} + 2 \cos 2\beta_{10}z' \right] \\
|H_{z2}|^2 &= \left| \frac{\pi}{a\omega\mu} \right|^2 |A^2| \cos^2 \frac{\pi y}{a} \\
&\quad \left[e^{-2\alpha_{10}z'} + e^{2\alpha_{10}z'} - 2 \cos 2\beta_{10}z' \right]
\end{aligned}
\quad \left. \vphantom{\begin{aligned} |E_{x2}|^2 \\ |H_{y2}|^2 \\ |H_{z2}|^2 \end{aligned}} \right\} \text{Region No. 2}$$

where

$$R = |R| e^{j\theta_r}$$

$$\Gamma_{10} = \alpha_{10} + j\beta_{10}$$

Value of A

Applying boundary conditions at the source:

Electric Current Source:

$$E_{x1}]_{z = -d_1} = E_{x2}]_{z' = -d_2}$$

$$A = \left[\begin{array}{c} \frac{-\Gamma_{10} d_1 + R e^{\Gamma_{10} d_1}}{e^{-\Gamma_{10} d_2} - e^{\Gamma_{10} d_2}} \\ \frac{-2\alpha_{10} d_1 + |R|^2 e^{2\alpha_{10} d_1} + 2|R| \cos(2\beta_{10} d_1 + \theta_r)}{e^{-2\alpha_{10} d_2} + e^{2\alpha_{10} d_2} - 2|R| \cos(2\beta_{10} d_2)} \end{array} \right]$$

$$= \frac{\cosh 2\alpha_{10} d + \cos(2\beta_{10} d + \theta_r)}{\cosh 2\alpha_{10} d - \cos(2\beta_{10} d)} \left. \text{if } \left\{ \begin{array}{l} |R|^2 = 1 \\ d_1 = d_2 = d \end{array} \right\} \right\}$$

Magnetic Current Source

$$H_{y1}]_{z = -d_1} = H_{y2}]_{z' = -d_2}$$

$$A = \left[\begin{array}{c} \frac{-\Gamma_{10} d_1 - R e^{\Gamma_{10} d_1}}{e^{-\Gamma_{10} d_2} + e^{\Gamma_{10} d_2}} \\ \frac{-2\alpha_{10} d_1 + |R|^2 e^{2\alpha_{10} d_1} - 2|R| \cos(2\beta_{10} d_1 + \theta_r)}{e^{-2\alpha_{10} d_2} + e^{2\alpha_{10} d_2} + 2|R| \cos(2\beta_{10} d_2)} \end{array} \right]$$

$$|A|^2 = \frac{-2\alpha_{10} d_1 + |R|^2 e^{2\alpha_{10} d_1} - 2|R| \cos(2\beta_{10} d_1 + \theta_r)}{e^{-2\alpha_{10} d_2} + e^{2\alpha_{10} d_2} + 2|R| \cos(2\beta_{10} d_2)}$$

$$= \frac{\cosh 2\alpha_{10} d - \cos(2\beta_{10} d + \theta_r)}{\cosh 2\alpha_{10} d + \cos(2\beta_{10} d)} \left. \text{if } \left\{ \begin{array}{l} |R|^2 = 1 \\ d_1 = d_2 = d \end{array} \right\} \right\}$$

The values of M_0 and J_0 may be derived by applying boundary conditions on tangential H for the electric source and tangential E for the magnetic source.

Radiated Power:

$$\text{Radiated power} = \text{Re} \int \int_{\text{aperture}} (\mathbf{E}_x \times \mathbf{H}_y^*) \cdot \hat{\mathbf{z}} \, dx \, dy$$

$$E_x = (1 + R) \sin \frac{\pi y}{a}$$

$$H_y^* = \left(\frac{k^2 a^2 - \pi^2}{a^2} \right)^* \left(\frac{-1}{j\omega\mu} \right)^* \left(\frac{1 - R^*}{\Gamma_{10}^*} \right) \sin \frac{\pi y}{a}$$

$$\text{Radiated power} = \text{Re} \left[(1 + R) (1 - R^*) \left(\frac{k^2 a^2 - \pi^2}{a^2} \right)^* \left(\frac{+1}{j\omega\mu^*} \right) \frac{1}{\Gamma_{10}^*} \right] \frac{ab}{2}$$

where:

$$\Gamma_{10}^* = \frac{1}{a} \left[\sqrt{\pi^2 - k^2 a^2} \right]^*$$

$$(\omega\mu a)^* = (ka) \left[\sqrt{\frac{\mu}{\epsilon}} \right] \left[\frac{\mu^*}{\mu} \right]$$

R = complex aperture reflection coefficient

$$ka = k_0 a \sqrt{(\mu_r' \epsilon_r' - \mu_r'' \epsilon_r'') - j(\mu_r' \epsilon_r'' + \mu_r'' \epsilon_r')}$$

$$\mu_r = \mu_r' - j\mu_r''$$

$$\epsilon_r = \epsilon_r' - j\epsilon_r''$$

$$\mu = \mu_r \mu_0$$

$$\epsilon = \epsilon_r \epsilon_0$$

It should be noted that the proper definition of the square roots must be chosen so that all the quantities have the correct physical significance. Γ_{10} is in the first quadrant, $(\omega\mu a)^*$ and ka are in the fourth quadrant for a time dependence $e^{j\omega t}$.

$$\text{Efficiency} = \frac{P_r}{P_r + P_L}$$

$$\begin{aligned} \text{where } P_L = & \omega \epsilon'' \int \int \int_{\text{cavity}} |E_x|^2 dv + \omega \mu'' \int \int \int_{\text{cavity}} [|H_y|^2 + |H_z|^2] dv \\ & + R_s \int \int_{\text{walls}} |H_{\text{tang}}|^2 da \end{aligned}$$

The following integration formulas are useful:

$$\begin{aligned} \int_0^{-d} [e^{-2\alpha_{10}z} + |R|^2 e^{2\alpha_{10}z} \pm |R| \cos(2\beta_{10}z + \theta_r)] dz \\ = \frac{1}{2\alpha_{10}} \left[|R|^2 e^{-2\alpha_{10}d} - e^{2\alpha_{10}d} + (1 - |R|^2) \right] \mp \\ \frac{|R|}{\beta_{10}} [\sin(2\beta_{10}d - \theta_r) + \sin \theta_r] \end{aligned}$$

$$\begin{aligned} \int_0^{-d} \left[e^{-2\alpha_{10}z} + e^{2\alpha_{10}z} \pm 2 \cos 2\beta_{10}z \right] dz \\ = \frac{1}{2\alpha_{10}} \left[e^{-2\alpha_{10}d} - e^{2\alpha_{10}d} \right] \mp \frac{1}{\beta_{10}} \sin 2\beta_{10}d \\ = \frac{-\sinh 2\alpha_{10}d}{\alpha_{10}} \mp \frac{\sin 2\beta_{10}d}{\beta_{10}} \end{aligned}$$

Magnetic Volume Losses

$$\begin{aligned} \omega \mu'' \int \int \int_{\text{cavity}} [|H_{y1}|^2 + |H_{y2}|^2 + |H_{z1}|^2 + |H_{z2}|^2] dv \\ = \textcircled{1} + \textcircled{2} + \textcircled{3} + \textcircled{4} \end{aligned}$$

$$\omega \mu'' a = |ka| \cdot \left| \sqrt{\frac{\mu}{\epsilon}} \right| \cdot \left| \frac{\mu''}{\mu} \right|$$

$$|\Gamma_{10}|^2 = \frac{1}{a^2} |k^2 a^2 - \pi^2|$$

$$|\omega \mu a| = |ka| \left| \sqrt{\frac{\mu}{\epsilon}} \right|$$

$$\textcircled{1} = \frac{|k^2 a^2 - \pi^2| \cdot \left| \sqrt{\frac{\epsilon}{\mu}} \right| \cdot \left| \frac{\mu''}{\mu} \right|}{|ka|} \frac{b}{2}$$

$$\left\{ \frac{1}{2\alpha_{10}} \left[|R|^2 e^{-2\alpha_{10}d_1} - e^{2\alpha_{10}d_1} + (1 - |R|^2) \right] + \frac{|R|}{\beta_{10}} \left[\sin(2\beta_{10}^{-\theta}) + \sin \theta_r \right] \right\}$$

$$\textcircled{2} = \frac{|A|^2 \cdot |k^2 a^2 - \pi^2| \cdot \left| \sqrt{\frac{\epsilon}{\mu}} \right| \cdot \left| \frac{\mu''}{\mu} \right|}{|ka|} \frac{b}{2} \left\{ \frac{-\sinh 2\alpha_{10}d_2}{\alpha_{10}} - \frac{\sin 2\beta_{10}d_2}{\beta_{10}} \right\}$$

$$\textcircled{3} = \frac{\pi^2 \left| \sqrt{\frac{\epsilon}{\mu}} \right| \cdot \left| \frac{\mu''}{\mu} \right|}{|ka|} \frac{b}{2} \left\{ \frac{[|R|^2 e^{-2\alpha_{10}d_1} - e^{2\alpha_{10}d_1} + (1 - |R|^2)]}{2\alpha_{10}} \right.$$

$$\left. - \frac{|R|}{\beta_{10}} [\sin(2\beta_{10}d_1 - \theta_r) + \sin \theta_r] \right\}$$

$$\textcircled{4} = \frac{|A|^2 \pi^2 \left| \sqrt{\frac{\epsilon}{\mu}} \right| \cdot \left| \frac{\mu''}{\mu} \right|}{|ka|} \frac{b}{2} \left\{ \frac{-\sinh 2\alpha_{10}d_2}{\alpha_{10}} + \frac{\sin 2\beta_{10}d_2}{\beta_{10}} \right\}$$

Electric Volume Losses

$$\omega \epsilon'' \iiint \left[|E_{x1}|^2 + |E_{x2}|^2 \right] dv$$

$$\omega \epsilon'' a = |ka| \cdot \left| \sqrt{\frac{\epsilon}{\mu}} \right| \cdot \left| \frac{\epsilon''}{\epsilon} \right|$$

$$= |ka| \cdot \sqrt{\frac{\epsilon}{\mu}} \cdot \left| \frac{\epsilon''}{\epsilon} \right| \frac{b}{2} \left\{ \frac{1}{2\alpha_{10}} \left[|R|^2 e^{-2\alpha_{10}d_1} - e^{2\alpha_{10}d_1} + (1 - |R|^2) \right] \right.$$

$$\left. - \frac{R}{\beta_{10}} [\sin(2\beta_{10}d_1 - \theta_r) + \sin \theta_r] \right\}$$

$$+ |A|^2 |ka| \cdot \left| \sqrt{\frac{\epsilon}{\mu}} \right| \cdot \left| \frac{\epsilon''}{\epsilon} \right| \frac{b}{2} \left\{ \frac{-\sinh 2\alpha_{10} d_2}{\alpha_{10}} + \frac{\sin 2\beta_{10} d_2}{\beta_{10}} \right\}$$

Surface Resistivity Losses

$$\begin{aligned} R_s \int_{\text{wall}} \int |H_{\text{tang}}|^2 da &= 2R_s \int_{\text{top wall}} \int \left[|H|^2 + |H_z|^2 \right] dy dz \\ &+ 2R_s \int_{\text{side wall}} \int |H_z|^2 dx dz \\ &= 2R_s \int_{\text{top wall}} \int \left[|H_{y1}|^2 + |H_{y2}|^2 + |H_{z1}|^2 + |H_{z2}|^2 \right] dy dz \\ &+ 2R_s \int_{\text{side wall}} \int \left[|H_{z1}|^2 + |H_{z2}|^2 \right] dx dz = \left[\textcircled{1} + \textcircled{2} + \textcircled{3} + \textcircled{4} \right] \\ &+ \left[\textcircled{5} + \textcircled{6} \right] \\ \textcircled{1} &= \frac{R_s |k^2 a^2 - \pi^2| \cdot \left| \frac{\epsilon}{\mu} \right|}{|k^2 a^2|} (a) \left\{ \frac{1}{2\alpha_{10}} \left[|R|^2 e^{-2\alpha_{10} d_1} - e^{2\alpha_{10} d_1} + (1 - |R|^2) \right] \right. \\ &\quad \left. + \frac{|R|}{\beta_{10}} [\sin(2\beta_{10} d_1 - \theta_r) + \sin \theta_r] \right\} \\ \textcircled{2} &= \frac{|A|^2 R_s |k^2 a^2 - \pi^2| \cdot \left| \frac{\epsilon}{\mu} \right| a}{|k^2 a^2|} \left\{ \frac{-\sinh 2\alpha_{10} d_2}{\alpha_{10}} - \frac{\sin 2\beta_{10} d_2}{\beta_{10}} \right\} \\ \textcircled{3} &= \frac{\pi^2 R_s \left| \frac{\epsilon}{\mu} \right| a}{|k^2 a^2|} \left\{ \frac{1}{2\alpha_{10}} \left[|R|^2 e^{-2\alpha_{10} d_1} - e^{2\alpha_{10} d_1} + (1 - |R|^2) \right] \right. \\ &\quad \left. - \frac{|R|}{\beta_{10}} [\sin(2\beta_{10} d_1 - \theta_r) + \sin \theta_r] \right\} \\ \textcircled{4} &= \frac{|A|^2 \pi^2 R_s \left| \frac{\epsilon}{\mu} \right| a}{|k^2 a^2|} \left\{ \frac{-\sinh 2\alpha_{10} d_2}{\alpha_{10}} + \frac{\sin 2\beta_{10} d_2}{\beta_{10}} \right\} \\ \textcircled{5} &= \frac{2\pi^2 R_s \left| \frac{\epsilon}{\mu} \right| b}{|k^2 a^2|} \left\{ \frac{1}{2\alpha_{10}} \left[|R|^2 e^{-2\alpha_{10} d_1} - e^{2\alpha_{10} d_1} + (1 - |R|^2) \right] \right. \end{aligned}$$

$$- \frac{|R|}{\beta_{10}} \left[\sin(2\beta_{10}d_1 - \theta_r) + \sin \theta_r \right] \Big\}$$

$$\textcircled{6} = \frac{|A|^2 \frac{2\pi^2 R_s}{|k^2 a^2|} \left| \frac{\epsilon}{\mu} \right| b}{\left\{ \frac{-\sinh 2\alpha_{10}d_2}{\alpha_{10}} + \frac{\sin 2\beta_{10}d_2}{\beta_{10}} \right\}}$$

2.5.2 Efficiency Using High Q Material. Certain simplifications to the above formulation can be made in some cases. If the loss tangent of the material is small enough so that $e^{\alpha_{10}d_1}$, $e^{\alpha_{10}d_2}$ are nearly unity, then the cavity fields can be represented by unattenuated exponentials for purposes of calculating losses in the cavity. The power radiated can be calculated simply by multiplying the power flow in the incident wave by $(1 - |R|^2)$. The problem will be reformulated using these assumptions. It should be noted that the assumption of unattenuated exponentials will hold if the loss tangent is sufficiently low even in cases where a low efficiency may result due to the high reflection coefficient.

$$\left. \begin{aligned} |E_{x1}|^2 &= \sin^2 \frac{\pi y}{a} \left[1 + |R|^2 + 2|R| \cos(2\beta_{10}z + \theta_r) \right] \\ |H_{y1}|^2 &= \frac{k^2 a^2 - \pi^2}{k^2 a^2} \frac{\epsilon}{\mu} \sin^2 \frac{\pi y}{a} \\ &\quad [1 + |R|^2 - 2|R| \cos(2\beta_{10}z + \theta_r)] \\ |H_{z1}| &= \frac{\pi^2}{k^2 a^2} \frac{\epsilon}{\mu} \cos^2 \frac{\pi y}{a} \\ &\quad \left[1 + |R|^2 + 2|R| \cos(2\beta_{10}z + \theta_r) \right] \end{aligned} \right\} \text{Region No. 1}$$

$$\left. \begin{aligned} |E_{x2}|^2 &= 2|A|^2 \sin^2 \frac{\pi y}{a} (1 - \cos 2\beta_{10}z') \\ |H_{y2}|^2 &= 2|A|^2 \frac{k^2 a^2 - \pi^2}{k^2 a^2} \frac{\epsilon}{\mu} \sin^2 \frac{\pi y}{a} (1 + \cos 2\beta_{10}z') \\ |H_{z2}|^2 &= 2|A|^2 \frac{\pi^2}{k^2 a^2} \frac{\epsilon}{\mu} \cos^2 \frac{\pi y}{a} (1 - \cos 2\beta_{10}z') \end{aligned} \right\} \text{Region No. 2}$$

Radiated Power

$$\text{Radiated power} = [1 - |R|^2] \times \frac{\sqrt{k^2 a^2 - \pi^2}}{ka} \sqrt{\frac{\epsilon}{\mu}} \frac{ab}{2} = P_R$$

Electric Volume Losses

$$\begin{aligned} & \omega \epsilon'' \iiint \left[|E_{x1}|^2 + |E_{x2}|^2 \right] dv \\ &= ka \sqrt{\frac{\epsilon}{\mu}} \frac{\epsilon''}{\epsilon} \frac{ab}{2} \left\{ (1 + |R|^2) \frac{d_1}{a} - \frac{|R|}{\sqrt{k^2 a^2 - \pi^2}} [\sin(2\beta_{10} d_1 - \theta_r) + \sin \theta_r] \right\} \\ &+ |A|^2 ka \sqrt{\frac{\epsilon}{\mu}} \frac{\epsilon''}{\epsilon} ab \left\{ \frac{d_2}{a} - \frac{\sin 2\beta_{10} d_2}{2\sqrt{k^2 a^2 - \pi^2}} \right\} \end{aligned}$$

Magnetic Volume Losses

$$\begin{aligned} & \omega \mu'' \iiint \left[|H_{y1}|^2 + |H_{y2}|^2 + |H_{z1}|^2 + |H_{z2}|^2 \right] dv \\ &= \textcircled{1} + \textcircled{2} + \textcircled{3} + \textcircled{4} \\ \textcircled{1} &= \frac{k^2 a^2 - \pi^2}{ka} \sqrt{\frac{\epsilon}{\mu}} \frac{\mu''}{\mu} \frac{ab}{2} \left\{ (1 + |R|^2) \frac{d_1}{a} + \frac{|R|}{\sqrt{k^2 a^2 - \pi^2}} [\sin(2\beta_{10} d_1 - \theta_r) + \sin \theta_r] \right\} \\ \textcircled{2} &= |A|^2 \frac{k^2 a^2 - \pi^2}{ka} \sqrt{\frac{\epsilon}{\mu}} \frac{\mu''}{\mu} ab \left\{ \frac{d_2}{a} + \frac{\sin 2\beta_{10} d_2}{2\sqrt{k^2 a^2 - \pi^2}} \right\} \\ \textcircled{3} &= \frac{\pi^2}{ka} \sqrt{\frac{\epsilon}{\mu}} \frac{\mu''}{\mu} \frac{ab}{2} \left\{ (1 + |R|^2) \frac{d_1}{a} - \frac{|R|}{\sqrt{k^2 a^2 - \pi^2}} [\sin(2\beta_{10} d_1 - \theta_r) + \sin \theta_r] \right\} \\ \textcircled{4} &= |A|^2 \frac{\pi^2}{ka} \sqrt{\frac{\epsilon}{\mu}} \frac{\mu''}{\mu} ab \left\{ \frac{d_2}{a} - \frac{\sin 2\beta_{10} d_2}{2\sqrt{k^2 a^2 - \pi^2}} \right\} \end{aligned}$$

Surface Resistivity Losses

$$\begin{aligned}
& 2R_s \int \int [|H_{y1}|^2 + |H_{y2}|^2 + |H_{z1}|^2 + |H_{z2}|^2] dy dz \\
& + 2R_s \int \int [|H_z|^2 + |H_{z2}|^2] dx dz = \textcircled{1} + \textcircled{2} + \textcircled{3} + \textcircled{4} + \textcircled{5} + \textcircled{6} \\
\textcircled{1} &= R_s \frac{k^2 a^2 - \pi^2}{k^2 a^2} \frac{\epsilon}{\mu} a^2 \left\{ (1 + |R|^2) \frac{d_1}{a} \right. \\
& \left. + \frac{|R|}{\sqrt{k^2 a^2 - \pi^2}} [\sin (2\beta_{10} d_1 - \theta_r) + \sin \theta_r] \right\} \\
\textcircled{2} &= 2|A|^2 R_s \frac{k^2 a^2 - \pi^2}{k^2 a^2} \frac{\epsilon}{\mu} a^2 \left\{ \frac{d_2}{a} + \frac{\sin 2\beta_{10} d_2}{2\sqrt{k^2 a^2 - \pi^2}} \right\} \\
\textcircled{3} &= R_s \frac{\pi^2}{k^2 a^2} \frac{\epsilon}{\mu} a^2 \left\{ (1 + |R|^2) \frac{d_1}{a} - \right. \\
& \left. \frac{|R|}{\sqrt{k^2 a^2 - \pi^2}} [\sin (2\beta_{10} d_1 - \theta_r) + \sin \theta_r] \right\} \\
\textcircled{4} &= 2|A|^2 R_s \frac{\pi^2}{k^2 a^2} \frac{\epsilon}{\mu} a^2 \left\{ \frac{d_2}{a} - \frac{\sin 2\beta_{10} d_2}{2\sqrt{k^2 a^2 - \pi^2}} \right\} \\
\textcircled{5} &= 2R_s \frac{\pi^2}{k^2 a^2} \frac{\epsilon}{\mu} ab \left\{ (1 + |R|^2) \frac{d_1}{a} - \right. \\
& \left. \frac{|R|}{\sqrt{k^2 a^2 - \pi^2}} [\sin (2\beta_{10} d - \theta_r) + \sin \theta_r] \right\} \\
\textcircled{6} &= 4|A|^2 R_s \frac{\pi^2}{k^2 a^2} \frac{\epsilon}{\mu} ab \left\{ \frac{d_2}{2} - \frac{\sin 2\beta_{10} d_2}{2\sqrt{k^2 a^2 - \pi^2}} \right\}
\end{aligned}$$

2. 5. 3 Efficiency with Probe Near Aperture. If the probe is located near the

aperture, the problem can be simplified to a single region.

Let $\Pi_y^* = \frac{1}{\beta_{10}} \left(\frac{-1}{j\omega\mu} \right) \cos \beta_{10} z' \sin \frac{\pi y}{a}$

$$E_x = j\omega\mu \frac{\partial \Pi^*}{\partial z} = \sin \beta_{10} z' \sin \frac{\pi y}{a}$$

$$|E_x|^2 = \sin^2 \beta_{10} z' \sin^2 \frac{\pi y}{a}$$

$$H_y = \frac{j\sqrt{k^2 a^2 - \pi^2}}{ka} \sqrt{\frac{\epsilon}{\mu}} \cos \beta_{10} z' \sin \frac{\pi y}{a}$$

$$|H_y|^2 = \frac{k^2 a^2 - \pi^2}{k^2 a^2} \left(\frac{\epsilon}{\mu} \right) \cos^2 \beta_{10} z' \sin^2 \frac{\pi y}{a}$$

$$H_z = \frac{-j\pi}{ka} \sqrt{\frac{\epsilon}{\mu}} \sin \beta_{10} z' \cos \frac{\pi y}{a}$$

$$|H_z|^2 = \frac{\pi^2}{k^2 a^2} \left(\frac{\epsilon}{\mu} \right) \sin^2 \beta_{10} z' \cos^2 \frac{\pi y}{a}$$

Radiated power

$$= (1 - |R|^2) \operatorname{Re} \int_0^a \int_0^b E_x H_y^* dx dy = (1 - |R|^2) \frac{ab}{8} \frac{\sqrt{k^2 a^2 - \pi^2}}{ka} \sqrt{\frac{\epsilon}{\mu}} = \bar{P}_r$$

Electric Volume Losses

$$\omega\epsilon'' \int \int \int_{\text{cavity}} \sin^2 \beta_{10} z' \sin^2 \frac{\pi y}{a} dv = \omega\epsilon'' \frac{a^2 b}{8} \left[\frac{2d}{a} - \frac{\sin^2 \beta_{10} d}{\sqrt{k^2 a^2 - \pi^2}} \right]$$

Magnetic Volume Losses

$$\omega\mu'' \int \int \int_{\text{cavity}} [|H_y|^2 + |H_z|^2] dv = \frac{\omega\mu''}{k^2 a^2} \frac{a^2 b}{8} \frac{\epsilon}{\mu} \left[k^2 a^2 \left(\frac{2d}{a} \right) + \frac{\sin 2\beta_{10} d}{\sqrt{k^2 a^2 - \pi^2}} (k^2 a^2 - 2\pi^2) \right]$$

Resistive Wall Losses

$$\begin{aligned}
 R_s \int \int_{\text{all walls}} |H_{\text{tang}}|^2 da &= \frac{R_s}{k^2 a^2} \frac{a^2}{4} \frac{\epsilon}{\mu} \left[\left(\frac{2d}{a} \right) k^2 a^2 \right. \\
 &+ \left. \frac{\sin^2 \beta_{10} d}{\sqrt{k^2 a^2 - \pi^2}} (k^2 a^2 - 2\pi^2) \right] \\
 &+ \frac{\pi^2 R_s}{k^2 a^2} \frac{ab}{2} \frac{\epsilon}{\mu} \left[\left(\frac{2d}{a} \right) - \frac{\sin 2\beta_{10} d}{\sqrt{k^2 a^2 - \pi^2}} \right] \\
 &= \frac{R_s}{k^2 a^2} \frac{a^2}{4} \frac{\epsilon}{\mu} \left[\frac{2d}{a} (k^2 a^2 + \frac{2b}{a} \pi^2) + \frac{\sin 2\beta_{10} d}{\sqrt{k^2 a^2 - \pi^2}} (k^2 a^2 - 2\pi^2 - 2\pi^2 \frac{b}{a}) \right]
 \end{aligned}$$

For Magnetic Volume Losses Only:

$$\frac{\bar{P}_L}{\bar{P}_r} = \left(\frac{\mu''}{\mu'} \right) \frac{\left[k^2 a^2 \left(\frac{2d}{a} \right) + \frac{\sin 2\beta_{10} d}{\sqrt{k^2 a^2 - \pi^2}} (k^2 a^2 - 2\pi^2) \right]}{(1 - |R|^2) \sqrt{k^2 a^2 - \pi^2}}$$

For Electric Volume Losses Only:

$$\frac{\bar{P}_L}{\bar{P}_r} = \left(\frac{\epsilon''}{\epsilon'} \right) \frac{k^2 a^2 \left[\frac{2d}{a} - \frac{\sin 2\beta_{10} d}{\sqrt{k^2 a^2 - \pi^2}} \right]}{(1 - |R|^2) \sqrt{k^2 a^2 - \pi^2}}$$

For Resistive Wall Losses Only:

$$\frac{\bar{P}_L}{\bar{P}_r} = \frac{.00796 R_s \sqrt{\frac{\epsilon}{\mu_r}} \left(\frac{b}{a} \right) \left[\frac{2d}{a} (k^2 a^2 + \frac{2b}{a} \pi^2) + \frac{\sin 2\beta_{10} d}{\sqrt{k^2 a^2 - \pi^2}} (k^2 a^2 - 2\pi^2 - 2\pi^2 \frac{b}{a}) \right]}{ka (1 - |R|^2) \sqrt{k^2 a^2 - \pi^2}}$$

Using these theoretical results, calculations of efficiency will be made and compared with the results of experimental efficiency measurements now in progress.

2.6 Design of Wideband Antenna Utilizing Ferrite

Design studies have been undertaken to enable the fabrication of a relatively broad band antenna combining the best features of the ferrite filled antenna family and the

traveling wave antenna family. The goal is to obtain an antenna operating satisfactorily over at least a 3 to 1 frequency range.

Design calculations are being centered on the modification of a backward traveling wave antenna. In this way the presence of ferrite has the least influence on the shortest waves where the ferrite is not necessary anyway. This procedure relaxes the requirements on the ferrite material and also shows some promise of higher efficiency.

Currently the studies are focused on the adaptation of the cavity-backed log conical antenna with ferrite loading. Preliminary experiments will be run on two and three layer ferrite loadings. One of the layers will be air with a polyfoam structure containing the air in cells. Beneath such a layer one or two more layers of either ferrite or dielectric will be used, perhaps both. It is anticipated that the first design will be described in the next bi-monthly report.

3. ACTIVITIES FOR THE NEXT PERIOD

The variational data for the admittance of a rectangular waveguide radiator will be expanded and a higher order mode correction will be added in a few cases. The experimental check of the variational results using the Emerson and Cumming slotted dielectric will be completed.

Efficiency measurements will be made on the rectangular cavity slot antenna loaded with powdered ferrite and compared with theoretical calculations. Beam patterns will be taken to determine the effect, if any, of feed arrangement on beam pattern.

Experimental work on the solid dielectric and solid ferrite rectangular cavity models will be started during the next period.

Aluminum castings have been ordered for the final model of the ferrite-powder-loaded rectangular cavity slot antenna.

SUMMARY

Theoretical curves for the input admittance of a rectangular waveguide radiator are presented. Equipment for an experimental check on this data for the particular case of $\mu = 1$, $\epsilon = 10$ has been completed.

The variational data has been used in a simple equivalent circuit representation which allows prediction of short position and bandwidth. Results from this method are compared with experimental data on short position and bandwidth from a ferrite-powder-loaded rectangular cavity slot antenna.

The variational data has been used in a calculation of efficiency. The formulation is presented; data will be given in the next report.

REFERENCES

1. R. F. Harrington, "Time Harmonic Electromagnetic Fields," McGraw Hill, 1961, p. 24.